Molecular Crystals and Liquid Crystals

Publication details, including instructions for authors and subscription information:
http://www.tandfonline.com/loi/gmcl20

Light Depolarization Effect by Electrohydrodynamic Turbulence in Nematic Liquid Crystals

C. Vena [a], C. Versace [a], G. Strangi [a], V. Bruno [a], N. Scaramuzza [a] & R. Bartolino [a]

[a] Centro di Eccellenza MIUR CEMIF.CAL, INFM-LICRYL Laboratory, Department of Physics and Università della Calabria, Rende, Cosenza, Italy

Version of record first published: 17 Oct 2011

To cite this article: C. Vena, C. Versace, G. Strangi, V. Bruno, N. Scaramuzza & R. Bartolino (2005): Light Depolarization Effect by Electrohydrodynamic Turbulence in Nematic Liquid Crystals, Molecular Crystals and Liquid Crystals, 441:1, 1-11

To link to this article: http://dx.doi.org/10.1080/154214091009464

Mol. Cryst. Liq. Cryst., Vol. 441, pp. 1–11, 2005

ISSN: 1542-1406 print/1563-5287 online
DOI: 10.1080/154214091009464

Taylor & Francis
Taylor & Francis Group

Light Depolarization Effect by Electrohydrodynamic Turbulence in Nematic Liquid Crystals

C. Vena
C. Versace
G. Strangi
V. Bruno
N. Scaramuzza
R. Bartolino
Centro di Eccellenza MIUR CEMIF.CAL, INFM-LICRYL Laboratory, Department of Physics and Università della Calabria, Rende, Cosenza, Italy

A study of the depolarisation effect which occurs in a light beam passing through a thin homogenously oriented layer of nematic liquid crystal (N-(methoxybenzylidene)-4-butylaniline) driven to the turbulence by an external ac voltage is reported. The time behaviour of the transmitted light polarization degree (P) has been recorded for different values of both applied voltage and polarization of the incident light beam.

The features of the DSM's regimes strongly depend on the state of polarization of the probe light beam. In particular, the transition can be evidenced by looking at P when the incident states of polarization are oriented at different angles with respect to the liquid crystal anchoring direction. Although the DSM's transition was unambiguously characterized as a transition from a 2-D structured turbulence to a 3-dimensional turbulence (DSM2), our measurements emphasize that oriented turbulent structures coexist in the latter regime.

Keywords: dissipative systems; ellipsometry; nematic liquid crystals; polarimetry; turbulence

The authors thank Bruno DeNardo, Francesco Capizzano, and Carmine Prete for their technical aid. The present investigations have been done in the framework of the Italian MIUR research project "Piani di Potenziamento della Rete Scientifica e Tecnologica" Cluster No. 26-P4.

Address correspondence to C. Versace, Centro di Eccellenza MIUR CEMIF.CAL, INFM-LICRYL Laboratory, Department of Physics and Università della Calabria, 87036 Rende, Cosenza, Italy. E-mail: versace@fis.unical.it

1. INTRODUCTION

During the past decade electrohydrodynamic turbulence (EHCT) in nematic liquid crystals (NLC) have attracted the interest of a large number of scientists [1–4]. In particular, the transition between two different turbulent states called dynamic scattering modes (DSM's) has been intensively studied [5–7] in a planar aligned NLC cell. EHC has proved to be a good testing ground for theories on dynamics of dissipative systems [8] and recently some application as also been proposed [9–11]. In a previous paper [12] we reported a study of the DSM1 $\longleftrightarrow$ DSM2 transition performed by a division of amplitude photopolarimeter (DOAP) [13]. The time evolution of the degree of polarization [14] and the behaviour of the radiation entropy [15] of the transmitted light allowed us to interpret the transition as a decay from a two-dimensional (DSM1) to a three-dimensional (DSM2) turbulence.

Most recently we have assembled a most performing four detector photopolarimeter (FDP) [16], which allows most accurate measurements in case of low level light signal (i.e., in the DSM2). In this paper the polarization degree P of the light transmitted by the sample in both DSM states is reported for different polarization states of the incident light beam. The polarization degree is a measure of the decoherence effect induced by the NLC director variations in the radiation field components, light propagating through a random fluctuating media is depolarized by decorrelation of the phase of the electric field components and its degree of polarization decreases [15]. Thus P can be view as an order parameter for the radiation field and its time evolution contains further information on the NLC molecular director dynamics.

2. EXPERIMENTAL

2.1. The Experimental Setup

The experimental setup is shown in Figure 1. The light beam emitted by a linearly polarized He-Ne laser (S) is transformed into a circularly polarized beam by the quarter wave retarder (R1), which is oriented at 45° with respect to the linear polarizer P2, so that the intensity of the beam can be varied rotating the polarizer P1 without changing its polarization.

The second polarizer-retarder couple (P, R) is used to transform the incident circular polarization into an arbitrary polarization state and two computer controlled motors allow to automatically select the polarizations states needed during the FDP calibration. The light

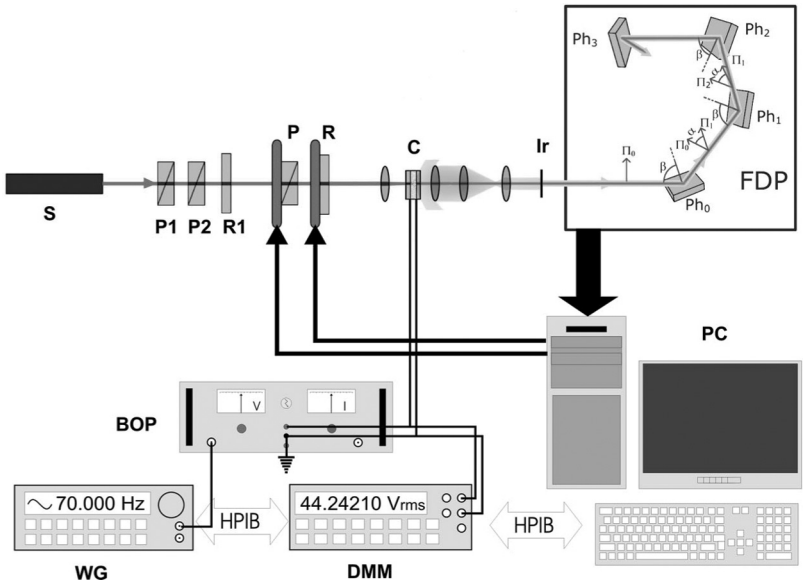

FIGURE 1 The experimental setup. S: 7 mW He-Ne laser. P1: dichroic linear polarizer. P2: Glan-Thompson linear polarizer. R1: multiple order quarter wave retarder, P: polarcor® linear polarizers. R: zero order quarter wave retarder. C: sample cell. Ir: 0.7 mm iris. FDP: photopolarimeter. WG: wave form generator. DMM: digital multimeter. BOP: bipolar operational amplifier. PC: personal computer.

beam emerging from the retarder R is focalized into the liquid crystal sample (C) and the transmitted light is collected and collimated into the photopolarimeter (FDP) by a three lenses system.

The temperature of the sample cell is controlled within $\pm 0.1^{\circ}$C by an electric oven (Instec RTC1) which is not shown in figure.

The applied voltage and the sample temperature are controlled through the HPIB bus by a personal computer (PC), which also hosts the FDP acquisition system (National AT MIO 16E-2 DAC card with the simultaneous sample and hold accessory SC-2040).

The FDP allows the simultaneous measurements of the four components of the Stokes vector $\vec{S} = (S_1, S_2, S_3, S_4)$ which completely characterizes the polarization state of a fully or partially polarized light beam. Then P is calculated by the relation:

$$P = \sqrt{\frac{S_1^2}{S_2^2 + S_3^2 + S_4^2}}$$

The FDP makes use of the reflections from four flat air-silicon interfaces provided by four windowless photodiodes (Hamamatsu S3590) to analyze the light polarization. As shown in Figure 1, the light beam impinges on the three first photodiodes at the Brewster angles ($\beta \sim 65^{\circ}$) and near the normal incidence on the fourth photodiode, furthermore the incidence plane Π is rotated of $\alpha \sim 45^{\circ}$ after each reflection. Under this conditions and supposing a linear response by the photodiodes the components S_i of the Stokes vector $\vec{S}$ can be obtained as linear combination of the four photocurrents I_i,

$$S_i = A_{i1}I_1 + A_{i2}I_2 + A_{i3}I_3 + A_{i4}I_4, \quad i = 1, \ldots, 4$$

or, casting the four photocurrent I_i in a column vector $\vec{I}$ and introducing the calibration matrix $\mathbf{A} = A_{ik}$,

$$\vec{S} = \mathbf{A}\vec{I} \tag{1}$$

The matrix $\mathbf{A}$ represents the inverse matrix of the Mueller matrix of the FDP, thus it must be experimentally determined by the calibration procedure every time the optical setup alignment is slightly modified. At least four polarization states, which correspond at four known independent Stokes vectors $\vec{S}_k$, must be used to calibrate the FDP [17]. According to Ref. [18], we got the best results selecting a circular polarization state (either left-handed or right-handed) and the three corresponding right-handed (left-handed) polarization states which define the largest tetrahedron inscribed in the Poincarè sphere (see Fig. 2).

During the calibration, for each polarization $\vec{S}_k$ of the incident light beam the corresponding photocurrents I_{lk} ($l = 1, 2, 3, 4$) are measured. If we indicate with S_{mk} the matrix whose columns are the four Stokes vectors we can calculate the calibration matrix by the relation $C_{lm} = I_{lk}(S_{mk})^{-1}$. Then, the Stokes vector $\vec{S}$ of every unknown polarization state can be determined by Eq. (1), where $A = C^{-1}$.

The calibration of the FDP has been tested measuring the ellipticity of the light emerging from the retarder R as long as the fast axis of R is rotated with respect to the transmission direction of the polarizer P. A typical result of a polarization run test in shown in Figure 3.

The liquid crystal cell (C) consisted in a commercially available (E.H.C. Co. Ltd.), 25 μm thick, sandwich-like planar cell (rubbed polyimide), which were filled by the N-(methoxybenzylidene)-4-butylaniline (MBBA) nematic liquid crystal (NLC). In our experiments we used also 8 μm and 50 μm thick cells without observing any substantial difference.

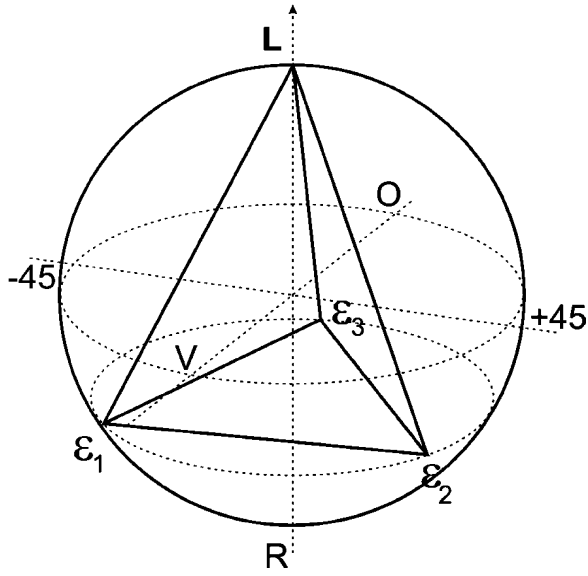

FIGURE 2 The Poincarè sphere, the polarization states $\vec{S}_k$ $(k = 1, 2, 3, 4)$ which correspond to the points L, $\varepsilon_1, \varepsilon_2$ and ε_3 have been selected to calibrate the FDP. L, $\varepsilon_1, \varepsilon_2, \varepsilon_3$ define the larger tetrahedron that can be inscribed in the sphere.

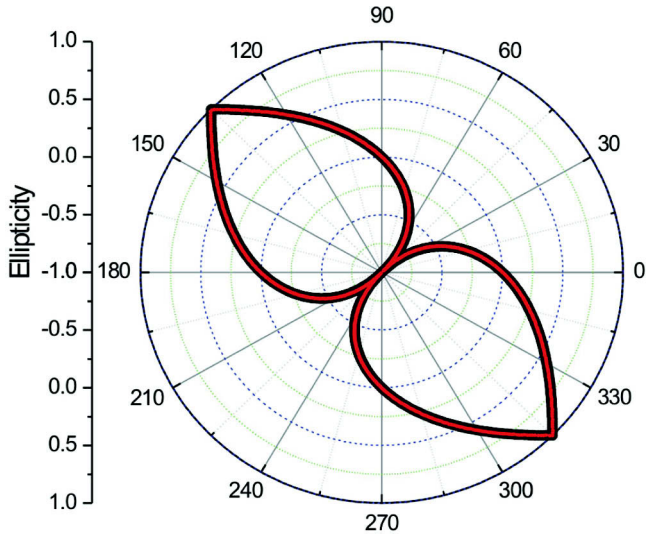

FIGURE 3 A FDP calibration test, the calculated (black points) and the measured (red points) light beam ellipticity is plotted as a function of the retarder (R) rotation angle.

2.2. Data Presentation and Discussion

The polarization state $\vec{S}$ of the light transmitted through the sample was determined by the FDP as long as a low frequency a.c. voltage V_0 was applied across the NLC layer.

Starting from the homogeneously planar oriented sample, as V_0 is increased, we observed at the onset of the electroconvenction the Williams-Kasputin rolls (Fig. 4a) then the "soft" turbulent regime (Fig. 4b, c) and a first turbulent regime (Fig. 4d), which is characterized by an intense and anisotropic scattering of light. The transition to a second turbulent regime (DSM2), which appears optically isotropic, occurs at highest voltages when the DSM2 areas nucleate in the DSM1 regime (Fig. 4e) and they enlarge to cover the whole sample (Fig. 4f).

In Figure 5 the time evolution of P is shown for three different polarization states of the incident light and four different r.m.s. values of $V_0 > V_{th}$.

In the DSM1 regime the degree of polarization P of the transmitted light is very sensitive to the incident polarization direction $\hat{p}_i$ for every applied voltage, light polarized along the alignment direction $\hat{n}_0$ is more depolarized than light polarized normally and P shows intermediate values if the incident polarization is circular. To minimize alignment

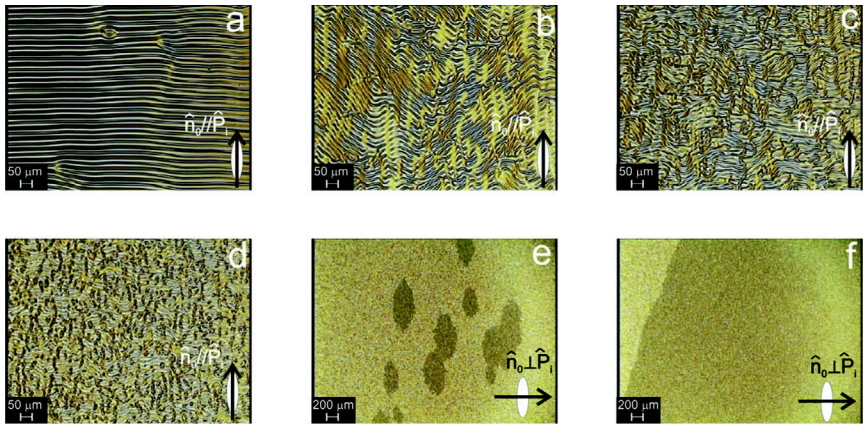

FIGURE 4 Images at the optical microscope of the electroconvective structures, $\hat{n}_0$ and $\hat{p}_i$ indicate respectively the anchoring direction and the polarization direction of the incident light, no analyzer as been used. a) the Williams-Kasputin electroconvective rolls ($V_a = 6.08$ volt). b) and c) fragmentation and bending of the rolls ($V_b = 9.0$ volt, $V_c = 11.0$ volt). d) the first turbulent regime DSM1 ($V_d = 22$ volts). e) and f) the transition to the second turbulent regime DSM2 ($V_e = V_f = 32$ volts), darkest DSM2 areas spread all over the sample.

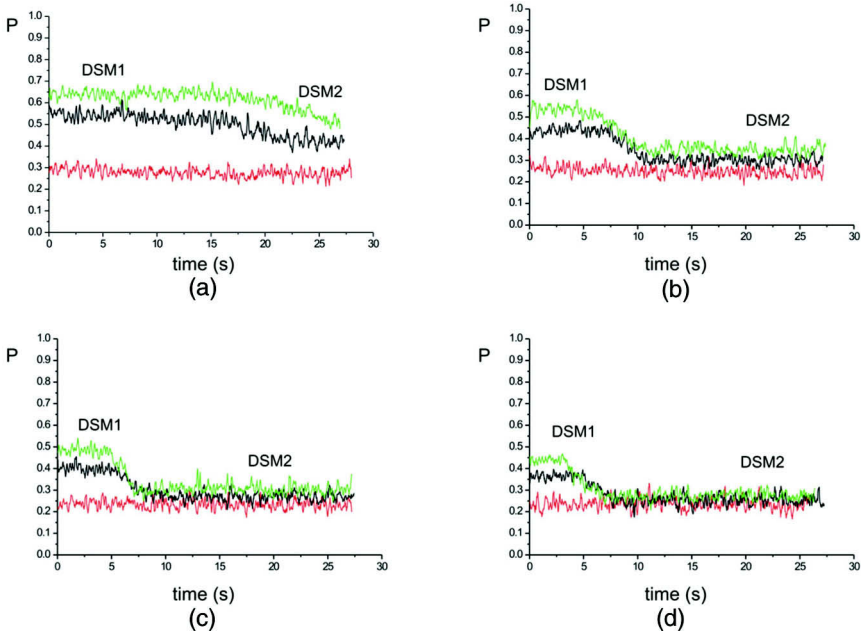

FIGURE 5 The degree of polarization P of the light transmitted by the sample vs. time for three different polarzations of the incident light beam (red: linear polarization parallel to the alignment direction $\hat{n}_0$; green: linear polarization normal $\hat{n}_0$; black: circular polarization) and four different applied a.c. voltages (a: 27 volt; b: 31 volt; c: 33 volt; d: 35 volt; all the voltages are r.m.s values).

errors, we repeated the measurements after having rotated the sample of π and we checked both left-handed and right-handed circular polarization, but we didn't observe any substantial difference. This behavior, which confirms the anisotropy of the DSM1, is consistent with previous observations (see for example Refs. [5,6,19]). On the contrary, the supposed isotropy of DSM2 is no longer valid if we look at P, in fact we have still observed a dependence on the incident polarization state and only at higher voltages the three curves in Figure 5 become indistinguishable.

This behavior is confirmed by data in Figure 6, where we report the averaged values of P in both DSM1 and DSM2 states as function of the applied voltage V_0. We note that, if $\hat{p}_i$ is directed along $\hat{n}_0$, P shows a slow linear dependence on V for both DSM states. While, if $\hat{p}_i$ is normal to $\hat{n}_0$ then we can observe a similar linear variation of P in the DSM1 followed by a stronger nonlinear decreasing in the DSM2.

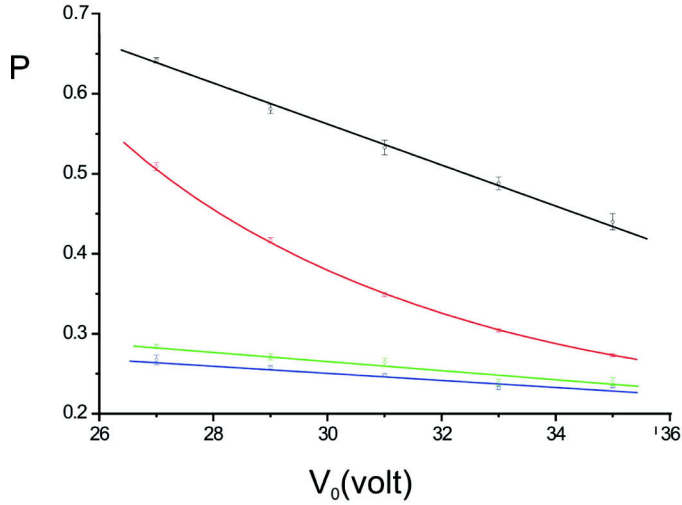

FIGURE 6 Polarization degree P of the transmitted light *vs*. the applied voltage V_0. Black: DSM1 and $\hat{p}_i \perp \hat{n}_0$. Red: DSM2 and $\hat{p}_i \perp \hat{n}_0$. Green DSM1 and $\hat{p}_i // \hat{n}_0$. Blue: DSM2 and $\hat{p}_i // \hat{n}_0$. Each point represents the average of P measured at a fixed voltage. Continuous lines are linear (black, green, blue) and exponential (red) regressions.

In Figure 7 we plot P *vs*. the applied voltage V_0 for different orientations of $\hat{p}_i$, in this case P is continuously measured while V_0 is slowly varied. In the DSM1 state, we can observe a drastic decrease of P when α, i.e., the angle between $\hat{p}_i$ and $\hat{n}_0$, tends to zero. When $\alpha \neq 0$, the transition to the DSM2 state is accompanied by a strong increase of the depolarization of the incident light, on the contrary, when $\alpha = 0$ we can observe a slight increase of P just at the DSM1 $\longleftrightarrow$ DSM2 transition, then P starts to decrease again as long as V_0 increases in the DSM2 state.

Finally in Figure 8 the polar graphic of P is reported as function of the azimuth angle of the incident linear polarization for different voltage values ($V_0 \in [33\,V,\ 39\,V]$) and both for DSM1 and DSM2 states. Semi-circles can be observed for each voltage and for both DSM1 (black) and DSM2 (red). The radius of each semicircle decreases when V_0 increases.

Data reported in Figure 8 highlight the anisotropy of both DSM's states. We can observe that the anisotropy reduces when the applied voltage is increased and P shows a dependence on the incident polarization angle even in the DSM2.

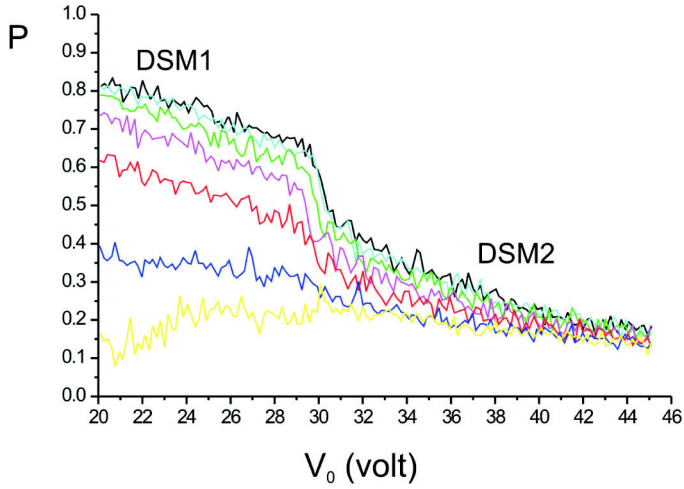

FIGURE 7 The polarization degree P of the transmitted light as a function of the applied voltage V_0 for different orientation α of the incident polarization $\hat{p}_i$ with respect to $\hat{n}_0$. Black: $\alpha = 90^\circ$, Cyan: $\alpha = 75^\circ$, Green: $\alpha = 60^\circ$, Pink: $\alpha = 45^\circ$, Red: $\alpha = 30^\circ$, Blue: $\alpha = 15^\circ$, Yellow: $\alpha = 0^\circ$.

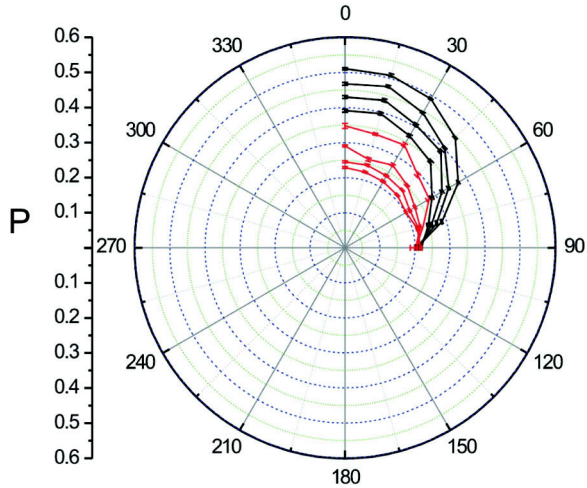

FIGURE 8 Polar graphic of P *vs*. the azimuth angle of the incident linear polarization for different $V_0 \in [33\,V,\ 39\,V]$. The radii of semicircles decrease when V_0 increases both for DSM1 (black semicircles) and DSM2 (red semicircles) states.

3. CONCLUSION

The polarization degree P of the light transmitted by the sample has been measured in the turbulent regimes which take place in a nematic liquid crystal layer under the action of an external ac voltage V_0. Different polarizations of the incident light have been used and we observed that P always decreases when V_0 increases. In the DSM1 state we revealed a strong dependence of the incident linear polarization on the direction $\hat{p}_i$: incident light polarized along the alignment direction $\hat{n}_0$ was strongly depolarized ($P \sim 0.2 \div 0.3$), when the angle between $\hat{p}_i$ and $\hat{n}_0$ tends to $\pi/2$ the depolarization decreases ($P \sim 0.6 \div 0.8$). We didn't observe any substantial difference for the circular polarization, which averages among the different $\hat{p}_i$ directions. A weak anisotropy has been still observed in the DSM2 state when the direction of $\hat{p}_i$ was varied, this anisotropy reduces as long as V_0 increases. Moreover, when $\hat{p}_i // \hat{n}_0$, an increase of P has been measured during the DSM1 $\longrightarrow$ DSM2 transition.

Our observations suggest that, according to previous observation, NLC molecular director chaotic oscillations are responsible for light depolarization in both DSM1 and DSM2, but while in the DSM1 state the directors can oscillate principally in a plane which contains the alignment direction (i.e., a plane orthogonal to the EHC rolls), in the DSM2 state the oscillations can develop also out of this plane. As a consequence, in the DSM1 areas can decorrelate only the component of the radiation field which is parallel to $\hat{n}_0$. The centers where these oscillations take place optically behave like abrupt changes of the media refractive so they can scatter and depolarize light. By increasing V_0 the number of these centers increases and a stronger light depolarization can be observed. Areas interested by the DSM2 state can decorrelate both components of the radiation electric field. At the transition there is not an abrupt increase of the number of scattering centers because V_0 has not been longer increased during the transition. This means that during the transition light polarized along $\hat{n}_0$ can experience a weaker depolarization. When V_0 is further increased in the DSM2 the total amount of defects increases and P decreases for all the polarization of the incident light beam. In other words we can imagine that DSM2 and DSM1 areas coexist after the transition, a further increase of the applied voltage causes the DSM1 areas to reduce their overall extension and, consequently, to increase that of the DSM2 areas.

This qualitative interpretation takes into account the observed phenomenology, further investigations are needed to get more insight on the origin and nature of the defects responsible for the light depolarization. In particular, an experimental setup that allows the

polarimetric study of the angular distribution of the scattered light in actually under construction. These measurements looking at the angular depolarization of both linearly and circularly polarized light would give information on the size of the turbulent domains which depolarize light.

REFERENCES

[1] Nasuno, S., Sasaki, O., Kai, S., & Zimmermann, W. (1992). *Phys. Rev. A*, *46*, 4954.
[2] John, T., Behn, U., & Stannarius, R. (2002). *Phys. Rev. E*, *65*, 046229.
[3] Funfschilling, D., Sammuli, B., & Dennin, M. (2003). *Phys. Rev. E.*, *67*, 016207.
[4] Komineas, S., Zhao, H., & Kramer, L. (2003). *Phys. Rev. E*, *67*, 031701.
[5] Kai, S. & Zimmermann, W. (1992). *Phys. Rev. A*, *46*, 4954.
[6] Kai, S. & Zimmermann, W. (1989). *Prog. Theor. Phys.*, *99*, 458.
[7] Toth-Katona, T. & Gleeson, J. (2004). *Phys. Rev. E*, *69*, 016302.
[8] Rosemberg, A. G., Hertrich, A., Kramer, L., & Pesch, W. (1996). *Phys. Rev. Lett.*, *25*, 4729.
[9] Coates, D. (1993). *Displays*, *14*, 94.
[10] Brugioni, S. & Meucci, R. (2003). *Optic. Comm.*, *216*, 453.
[11] Gleeson, J. T. (2002). *Appl. Phys. Lett.*, *81*, 1949.
[12] Strangi, G., Versace, C., Scaramuzza, N., Lucchetta, D. E., Carbone, V., & Bartolino, R. (1999). *Phys. Rev. E*, *59*, 5523.
[13] Azzam, R. M. A. (1982). *Optica. Acta.*, *29*, 685.
[14] Azzam, R. M. A. & Bashara, N. M. (1987). *Ellipsometry and Polarized Light*, North-Holland: Amsterdam.
[15] Brossau, C. & Bicout, D. (1994). *Phys. Rev. E*, *50*, 4997.
[16] Azzam, R. M. A. (1985). *Opt. Lett.*, *10*, 309.
[17] Brudzewski, K. (1991). *Journal of Modern Optics*, *38*, 889.
[18] Masetti, E. & Desilva, M. P. (1994). *Thin Solid Films*, *246*, 47.
[19] Kai, S., Zimmermann, W., Andoh, M., & Chizumi, N. (1990). *Phys. Rev. Lett.*, *64*, 1111.